University of Washington Master's in Earth and Space Sciences: Applied Geosciences (MESSAGe) Capstone Report

Chambers Creek, Pierce County, WA – Landslide Susceptibility Assessment

Deep and shallow-seated landslide susceptibility model

Aleksander Srebro

Cohort 6 MESSAGe Student

Abstract

In wet, glacially overridden regions, landsliding is a common and dangerous natural phenomenon. Thus, attempting to predict these mass wasting events is a vital and useful task. Many landslide models already exist, but the ultimate goal of this Capstone Project was to create a deep and shallow landslide susceptibility model of a segment of the right bank of Chambers Creek Basin. By combining field and computer testing, appropriate material strength values, potential slide plane slopes and depths, a factor of safety analysis, slope and curvature models, a vegetation analysis, and field observations a thorough deep and shallow landslide hazard model was created. According to the data, the highest risk of shallow landsliding is located in the center of the field area, within the Pre-Vashon non-glacial course-grained unit (A2). The highest risk of deep landsliding is located on the eastern extent of the field area, where a concave, protruding section sticks out into the valley (between the western face of the most eastern large landslide complex and where the Pre-Vashon till (C1) reaches the surface). Both models agreed that the lowest risk of both deep and shallow landsliding is located on the western edge of the field area, due to the exposure of the strong underlying Pre-Vashon non-glacial fine-grained unit (C2).

Acknowledgments

I would like to thank Professor Allison Duvall for her patience, constant proof reading and advising. I appreciate her determination with helping me finish my Capstone Project on time, which helped me graduate. I would also like to thank Professor Kathy Troost for accompanying my into the field and helping me better understand my field area and the processes that occur there. Finally, I would like to thank Professor Juliet Crider and all of my MESSAGe professors for teaching me all I needed to know for this project and preparing me as best they could for the professional world.

Table of Contents Page

Chambers Creek, Pierce County, WA – Landslide Susceptibility Assessment

Introduction

This report documents a deep and shallow landslide assessment of a segment of the river right bank of the Chambers Creek Basin in University Place, WA (Figure 1). Analysis of lidar imagery reveals that the right bank of the Chambers Creek Basin has experienced several shallow and deep-seated landslides in the past. These and future mass wasting events pose a threat to the homes and residents of the area. A shallow and deep-seated landslide assessment of the steep bank would allow the residents north of the hazard zone to implement mitigation methods if they are located in a highly susceptible area.

Apart from the dangers and damages commonly associated with a landslide event, excessive sediment delivery to Chambers Creek from landsliding could have a large negative impact on the flow and ecosystem of the river. Chambers Creek is a relatively narrow creek, with a cross-sectional distance of about 20 feet and a floodplain width between 250 and 400 feet. Thus, even a relatively small shallow or deep landslide could form a sediment dam and block the river. Such a dam could then cause water levels to rise and flood residential properties at or near the flood plain level. If the sediment dam were to then burst and a sudden increase in discharge were to occur, the sewer treatment plant downstream of the field site could sustain damage and deposit its waste into Puget Sound. This type of event would also increase the sediment load in the stream, which decreases water quality, and poses a threat to salmon populations that use the creek as a means of getting to their spawning grounds.

In 2017, Mickelson et al. (2017) published a general shallow and deep-seated landslide assessment completed by the Washington Geologic Survey (WGS). The county landslide hazard assessment revealed that the entire right bank of Chambers Creek is susceptible to both shallow and deep-seated landslides. Specifically, the data showed that the field area is highly susceptible to deep-seated landslides and moderately susceptible to shallow landslides. However, based on observations done over the years, I believe that the right bank is less susceptible to landsliding than determined by Mickelson et al. (2017), but also, that some homes may be more vulnerable than others. The data collect by Mickelson et al. was obtained only using lidar data of the region. This state landslide assessment did not take into account local features or conditions such as the underlying material density/strength, strike and dip of the underlying geologic units, perching water, or the stratigraphy of the area and possible slide planes.

To improve and build upon the work conducted by Mickelson et al. in 2017, the landslide analysis of the river right bank of the Chambers Creek Basin focused on the slope, curvature,

vegetation, geotechnical properties of the hillslope material (cohesion and angle of internal friction), and the stratigraphy of the field site to create a detailed, site-specific landslide susceptibility model. The data analysis, modeling, and presentation for this capstone project were done using a Geographic Information System (GIS). In addition, field work was conducted to determine geologic and geomorphic features and field tests were conducted to determine the material properties of the underlying units.

Background

Chambers Creek Basin

The field area is located on the river right bank of the Chambers Creek Basin, south of a populated neighborhood (Figure 2). The neighborhood contains 25 houses and has a population of about 75 people. On the eastern edge of the field site there is an old landslide deposit and scarp that has been converted into a park (Kobayashi Park). Chambers Creek is one of four subwatersheds that make up the Chambers Creek – Clover Creek watershed. Chambers Creek is a major surface water source in the watershed and is a year round stream draining about 12.8 mi^2. The creek originates at Steilacoom Lake and then flows north, joining Flett Creek and Leach Creek. From there the creek flows west down a 100-200-foot-deep valley and then discharges to Puget Sound. Like the majority of the south Puget Sound area, Chambers Creek Basin has relatively dry summers and cold winters with persistent rainfall for about half the year and an average rainfall of about 42 inches. The vegetation in the basin is composed primarily of tall evergreen trees, deciduous trees, blackberry and raspberry bushes, and various shrubs and water loving plants like horsetails.

Geologic Setting

As with most of western Washington, the geological history of the Chambers Creek Basin is correlated with periods of large scale glacial advance and retreat, separated by deposition and erosion during interglacial periods. Prior to the Last Glacial Maximum, sea level was as much as 490 feet lower than it is today (Bretz, 1910). As the glacier retreated, water from the Cascade and Olympic Mountains drained north through the Puget Lowland, eroding existing geologic material and depositing alternating layers of sand, silt, and clay, toped with gravel deposits along drainage channels as the water made its way to the Pacific Ocean. This repeated erosional and depositional event left a geologic stratigraphy containing many unconformities, multiple palotopographic surfaces, extensive channels and channel fills, different lithologies with many vertical and horizontal facies, and multiple discontinuities (Troost, 2008). Thus, we commonly find areas in the Puget Lowland covered with unconsolidated recessional material with glacial till underneath, overlying consolidated sands, gravels, silts, and clays.

In the Puget Lowland region, the glacier that came down from Canada is called the Puget Lobe. Once the Puget Lobe extended to Olympia, Lake Puyallup formed underneath the glacier. About 13,500 years before present, a series of multiple glacial outburst floods from glacial Lake Puyallup scoured the Chambers Creek Basin and the surrounding area during deglaciation in the Puget Lowland (Troost, 2007). Evidence for these large erosional events includes the lack of north-south drumlins; which can be found surrounding the scoured areas. These glacial outburst floods, or jökulhlaups, created a series of channels throughout the central Pierce County area and deposited the Steilacoom Gravel in the area. These large scouring events are a result of ice thinning over Glacial Lake Puyallup during deglaciation. The jökulhlaups produced a series of erosional and depositional terraces throughout the Lakewood, Tacoma, and University Place area, including the Chambers Creek Basin (Troost, 2007). In many places an unconformity exists between the Pre-Vashon deposits and the Vashon Recessional Outwash deposited by the jökulhlaups.

Landslides in the Puget Lowland

Landslides are common in the Puget Lowland for several reasons: steep topography, weak – and thus susceptible – geologic deposits and contacts, human interference, and abundant rain.

Steep topography plays a major role in driving landslides, and the likelihood of forming a landslide on one of these slopes increases if the slopes are converging (forming a hollow). This is due to the fact that terrestrial waters converge into the center of the hollow during a storm and thus increase the pore water pressure and erosional potential of the area. Even from simple slope models of the Puget Lowland, we can see that many of the coastal and river valley slopes in the Puget Lowland contain slopes greater than 40 degrees, which are the minimum slopes required to create shallow landslides.

Stratigraphy also plays an important role in slope stability, especially in glacially altered regions such as the Puget Lowland. In the field area, due to its glacial history, the majority of the surface is overlain by colluvium and Vashon recessional outwash. When terrestrial water percolates through the colluvial and outwash layers, it pools on top of the dense underlying glacial till, increasing the pore pressure between this layer and the overlying Vashon recessional outwash. When pore pressure increases, the material weakens due to a decrease in cohesion and friction between the grains. This saturated area can then host landslide failure planes.

Due to its destabilizing properties, water also plays a major role in this regions landslide history. River water meanders and cuts into the toes of slopes, destabilizing them further and making them more susceptible to mass wasting events. Precipitation rate and intensity influence how much water is present on and in the slope. Infiltration rate determines how fast the terrestrial water will be absorbed by the ground surface and whether or not overland flow and erosion will occur. Springs and seepages on slopes concentrate water in certain locations and change the

shape of the slope. Finally, groundwater influences the elevation, vertical extent of river systems, and amount of water in a region and on the slopes.

Other factors including slope aspect, human interference/construction, and vegetation on the slopes also play a role in determining slope stability. The aspect (Myers, 1993), or slope-facing direction, influences how much rain and sun exposure a slope receives. The slopes in the field area have a south facing aspect and thus receive more sunshine. Anthropogenic, or human, interferences can either strengthen or weaken slopes depending on what work is being performed. In landslide prone areas, changes in the age distribution of vegetation of an area can be used to determine a recurrence interval for landsliding, and older landslide deposits tend to have more vegetated and extensive vegetative canopies.

Current Pierce County Landslide Hazard Map

Based on lidar observations, and according to the Mickelson et al. (2017) inventory, landsliding has been occurring in this basin for over 150 years, but none have been officially reported to WGS or catalogued in the field area. Unfortunately, a detailed landslide history of the Chambers Creek Basin is not readily accessible or available. However, in the eight years that I have lived in the field area, I have found evidence for and also witnessed both deep-seated and shallow-seated landslides. A minor shallow slide occurred in 2012 and removed a single evergreen tree south of one of the homes on the river right bank of Chambers Creek. Based on my observations, shallow landslides have occurred about every two years.

The landslide inventory map created by Mickelson et al., (2017) utilized a fairly simple lidar based landslide susceptibility analysis. In this inventory, using the most current lidar imagery of the field area, the landslide deposits were identified along with their corresponding scarps (major and minor) and flanks (Figures 3a and b). Using the ESRI ArcGIS program, Mickelson et al. (2017) then calculated various characteristics (slope gradient, headscarp height, failure depth, landslide volume) for each mapped landslide deposit.

Methods

In order to take what was done for Pierce County (Mickelson et al., 2017) one step further, my Capstone project incorporated local conditions, geology, and orientation of geologic units into the landslide susceptibility analysis. I completed a landslide inventory for the field area where the average slope, landslide area, failure depth, and landslide cover and volume were calculated for each potential landslide deposit in the field area. Once this inventory was complete, a vegetation and surface material strength analysis was conducted to provide additional information about shallow landsliding in the field site, and a stratigraphic and subsurface material strength analysis was conducted to provide additional information about deep landsliding in the field area. All of these components were then used to create a factor of

safety model for deep and shallow-seated landsliding. This model was then combined with the information obtained from the NDVI model and field data/observations to assess landslide susceptibility.

Slope and Curvature Model

In the simplest landslide models, slopes that have a grade of 70 percent (40 degrees) or greater are considered possible landslide forming slopes. Thus the first step in creating a slope and curvature model in ArcGIS was to create a slope layer from the 2011 lidar (WDNR, Accessed 2018) data in degrees and displayed that data as a Bilinear IDW Interpolation due to the continuous nature of the data. Using the same lidar image a curvature assessment was then done and separated into a plan-and-profile view curvature raster. Using the following formula: ("slope">=70)*("smoothed plan curvature"<=-1), places that contained a slope greater than or equal 40 degrees and were concave in plan view were isolated. Forty degrees was chosen as the lower boundary since it is commonly used as the minimum slope for landsliding to occur, since the angle of repose for colluvial material lies between 30 and 40 degrees (Fleming and Johnson 1994).

Vegetation Analysis

In order to obtain some general information about the stability of the surface slopes in the area, a vegetation analysis was conducted. As stated in Myers (1993), there is a correlation between vegetation type and surface slope stability. Vegetation like deciduous trees (particularly alders) and blackberry bushes are the first to take root after mass wasting events. Most deciduous trees and blackberry bushes tend to have shallow but wide root systems and thus do not require stable slopes to grow. Evergreen trees, on the other hand, tend to have narrow but deep root systems and grow best in stable soils. Using this reasoning, a vegetation analysis can be used as a proxy for slope stability. In this Capstone project, it was assumed that the areas containing evergreen trees are less susceptible to shallow landsliding or have not failed in the last 150 years.

Using the reasoning above, the mapping of vegetation types in the field area, could reveal the sections of the river right bank slope that are more and less susceptible to shallow landsliding. Once these areas are identified, a scale factor (where deciduous = 1 and evergreen = 2) can be added to the shallow landslide susceptibility calculation in order to account for the root stabilizing factor.

In order to perform the vegetation analysis, a Normalized Difference Vegetation Index (NDVI) was conducted on the field area. NDVI's are primarily used to assess the health of vegetation in agriculture and forestry (GIS Geography, 2018). This GIS tool uses near-infrared and red light bands to distinguish between different plant types. Since deciduous trees lose their leaves during the winter months a multi-band high-resolution winter image of the field area was used. Once the multi-band image was obtained (GIS Image, Accessed 2018) the NDVI was created using the Image Analyst Tool in ArcGIS. Of the four bands available with the multi-band

winter image, Band 2 was used for the red and Band 4 was used for the infrared portion of the analysis. From the NDVI, areas containing evergreen trees and deciduous trees/shrubs were isolated by focusing on specific NDVI values that indicated lush, green terrain. The result of this analysis formed a raster polygon image that indicated areas of evergreen and deciduous trees. The data were then trimmed down and only the vegetation type in the basin was shown. This same process was attempted with a summer base image (where the deciduous trees contained their leaves) but the result was inaccurate and showed a lower percentage of evergreen trees than were actually present in the field area. The winter image results were then verified using field observations and were concluded to be a relatively accurate representation of the field area vegetation. Since deciduous trees are not the only seasonal plant in the basin, the areas identified as deciduous may not contain just deciduous trees but may include shrubs, bushes, and blackberries as well.

Properties of Slope Forming Materials

In order to obtain the necessary material properties to calculate factor of safety, measurements of surface and subsurface strength were conducted. The primary method used for the measurements was a modified version of a standard penetration test (SPT). Due to my inability to bring heavy machinery into the field, during the shallow SPT testing the modified standard penetration test consisted of first digging to a prescribed depth and then manually hammering a vertically oriented split spoon into the underlying unit. For the SPT testing a known weight of 8 pounds and known drop height of 18 inches were repeatedly dropped in free fall and tallied until the top of the 12 inch split-spoon was at unit level. During the standard penetration testing, the grain size and unique characteristics of the different geologic units were determined.

Surface Tests

For the surface (shallow) component of the SPT testing, a two to three foot ditch was dug into each colluvium test sites (to bypass the vegetation horizon). The sites were determined by locating areas with little vegetation cover, which had recently disturbed soils, and were at least 2 meters from any large trees. From these blow count (blows/foot) an N value was obtained, and then corrected using the Burmister correlation (Rodgers, 2006) to account for the modification in procedure. These corrected N values were then correlated with cohesion and angle of internal friction using tables from Holtz et al. (2011). This produced a range of cohesion and angle of internal friction values for the colluvial material that covers the slopes.

Subsurface Tests

The same process was repeated for the subsurface (deep) SPT testing except during this test the digging depth ranged from two to six feet depending on location (to bypass the colluvium and reach the native material). Once again, the modified standard penetration method was used to determine the subsurface cohesion and angle of internal friction. In this case, some of the data was obtained from the large landslide site to the east of the field area due to exposure of the

subsurface layers. Other sites were scattered across the field area and, due to access issues, were taken wherever an exposure was at or near the surface. For these tests all delineated units were tested in order to input the data into the factor of safety model. Once an N values were obtained, they were also corrected using the Burmister correlation (Rodgers, 2006) to account for the modification in procedure.

Combining Slope, Curvature, NDVI, and SPT Data

After completing the slope and curvature model, areas containing concave slope of greater than 40 degrees were isolated. A Bilinear IDW Interpolation was performed on both the NDVI data (as a scale factor) and surface SPT values and then a multi-variable overlay was performed between the slope-curvature, NDVI, and SPT data. By overlaying the slope-curvature model with the NDVI scale factor and the surface SPT values, areas along the river right bank that contained landslide forming slopes, with weak surface material and deciduous cover could be isolated. In addition, the overlay isolated areas that did not have landslide forming slopes, had stronger surface material, and were covered by evergreen trees. Finally, this overlay indicated areas that had the various combinations of (non-)landslide forming slopes, strong/weak surface material, and evergreen/deciduous cover.

Stratigraphic Data and Susceptible Geologic Contacts

Field mapping was undertaken to document the underlying stratigraphy and identify susceptible geologic contacts. The west scarp of the landslide in Kobayashi Park exposes geologic units that extend through the field area. In addition, while walking downriver observations of the right bank geology were made where outcrops could be found. Due to dense vegetation and colluvial cover, I make the simplifying assumption that the geologic units identified on the landslide scarp and along the river project into the main study area and are continuous. I also assume continuous unit thicknesses throughout the field area. After a rough geologic cross section of the field area was created, susceptible geologic contacts were determined by observing where seeps occur along the river right bank slope.

Deep and Shallow-Seated Landslide Factor of Safety Model

To create the factor of safety (FS) model, the FS equation below was used:

$$FS = \frac{Shear\ Stregth}{Shear\ Stress}$$

$$= \frac{C' + gz(\cos(\Theta))^2(\rho_s - \mathrm{m}\rho_w)\tan(\phi)}{(\rho_s gz)(\sin(\Theta)\cos(\Theta))}$$

In this equation C' is the effective cohesion, g is gravity, z is the vertical depth to the base of the slide plane, Θ is the slope, ρ_s is the density of the regolith, m is the wetness factor (percent of soil column saturates), ρ_W is the density of water, and ϕ is the angle of internal friction. This equation is commonly referred to as the 'infinite slope equation'. Under normal circumstances,

this equation is used to find the factor of safety for translational (shallow) slides, however, this equation was also used for the deep-seated landslide model. In order to apply this equation to a deep (curved) landslide scenario, the slope of the failure plane of the slide was divided into multiple segments that were treated as individual translational slide planes. This method is commonly referred to as the slice method. The average FS of these results was then taken to determine the factor of safety in that location. Utili and Nova (2007) demonstrated, using equations and field tests, that concave log-spiral slopes (like those of deep landslides) produce factor of safety results that are higher than those of planar slopes, thus the translational equation itself could not be used for the deep scenario.

By conducting the SPT test on the surface and subsurface layers found at the field site, the variables for the above equation were calculated and obtained. Once the variables were converted to the correct units, they were implemented into the above equation. This factor of safety calculation was conducted for both all susceptible geologic contacts in order to provide the most accurate factor of safety model of the field area. The factor of safety data were then cross referenced with the NDVI scale factor and the acquired SPT data to create a deep-seated factor of safety model.

Using the factor of safety equation above, and by converting the values to the appropriate units, a factor of safety calculation was done every 160 feet along the 2,200 feet long bank. These factor of safety calculation locations (Tables 3a and b) are organized so that they start on the eastern edge of the field area and move counterclockwise toward the western edge. In order to accurately display the factor of safety values, the height values were modified at each measured point to account for any dip in the subsurface geologic layers. In addition, the slope was modified at each point to account for changes in local slope.

To create the shallow susceptibility models, each location had a low and high factor of safety calculation to account for uncertainty in input variables and for seasonality (where summer is considered low and winter is considered high). The main difference between the two seasons is accounted for in the wetness factor (m) value in the factor of safety equation. Wetness values were chosen by observing average changes in stream level, rainfall data of the region, and groundwater measurements (USGS Stream) of Chambers Creek.

To create the deep susceptibility model, average values for the density, thickness, and slope of the material were combined using the slice method and the final results were then averaged to obtain a FS value for each factor of safety calculation location. In order to account for all possible slide planes, all susceptible geologic contacts were treated as separate slide planes and received their own calculations. In these calculations, the susceptible geologic contacts were assumed to be impermeable in order to make calculations simpler and not have to account for percolation. Finally, it was assumed that the cutoff for deep and shallow-seated landsliding is at 15 feet (Burns et al., 2009) which primarily consists of colluvium and the native material in contact with the colluvium.

Findings

NDVI, Slope, and Surface SPT

From the NDVI image (Figure 5) it was discovered that the right bank of Chambers Creek (from the western scarp of the eastern landslide deposit to the eastern bank of the tributary channel to the west) is comprised of about 72% evergreen threes and 28% deciduous vegetation. By overlaying the NDVI results with the slope map of the field area we see that steeper slopes are more often found in areas of evergreen trees (right bank), while shallower slopes are covered in deciduous trees (left bank). From this analysis, we see that evergreen trees are only found on the valley walls, while deciduous trees inhabit the flatter or recently disturbed areas. It is thus assumed that the areas containing evergreen trees are more stable and less likely to result in failure.

From the slope map (Figure 6) of the field area we can see that the river right bank of Chambers Creek in this area has slopes between 60 and 80 degrees. Even by looking at just the slope map, we can see that if 40 degrees is the minimum to produce landsliding then the entire river right banks of Chambers Creek is susceptible to at least shallow landsliding. In contrast, the river left bank has slopes ranging from 20 to 40 degrees.

From the surface SPT results, it was revealed that the strength of the artificial fill or colluvium on the right bank of the Chambers Creek Basin seems to increase (higher blows/ft) toward the western edge of the field area. This could either be due to a higher strength in material, bias associated with collecting only 35 measurements in the field area (Figure 7), and/or sampling in areas with low vegetation and having freshly exposed sediments (presumably already failed and the weakest part of the colluvium cover removed). The lowest N value in the colluvium was 1.12 blows per foot while the highest was 5.48 blows per foot (Table 1). From an average corrected N value of about 3.54 blows per foot a cohesion range of about 12-25 kPa and an angle of internal friction range of about 27-32 degrees was obtained. In addition, from the field observations and the two values stated previously, it was determined that the surface material has the consistency of loose soil. When this data is overlaid with the NDVI results, we see that areas covered in evergreen trees have higher surface N values then areas covered by deciduous trees (Figure 8). This distribution of SPT data could also be a proxy for landslide age, since the river right bank is covered in landslide deposits. Since a landslide deposit will become stronger as time passes, the areas with the lowest blows/foot in Figure 7 could indicate younger shallow surface slides while areas with higher blows/foot and evergreen cover could indicate older slide deposits. During field reconnaissance it was found that the colluvium is a mixture of artificial fill near the top of the slope, from the housing development upslope, and material eroded of the Vashon and Pre-Vashon units further downslope. This unit was very loose to loose and was primarily a mixture of sand and gravel with few cobbles and a variable silt content.

Stratigraphy

While conducting field work it was discovered that there are two possible susceptible geologic contacts and that the units in the field area are dipping about 4 degrees to the east southeast. Directly underneath the veneer of colluvium and artificial fill layers is a Vashon recessional outwash unit that is primarily a loose to medium dense sand with gravel and some cobbles (unit A1, Table 2). Underneath this layer is a very dense Pre-Vashon glacial till that is primarily composed of gravel sized sediment in a fine-grained matrix (C1). Underneath the Pre-Vashon till is a very dense, coarse-grained Pre-Vashon non-glacial sandy unit (A2) underlain by a very dense to hard fine-grained version of the same non-glacial unit (C2). The two possible susceptible geologic contacts lie where units A1 and C1 connect and where units A2 and C2 connect (Figure 9a). Direct evidence for contact susceptibility presented itself in the form of large seeps above unit C1 and smaller seeps above unit C2 even though field work was conducted in mid-July. The geologic units and some of their properties are summarized in Table 2. The surface and subsurface units are shown in Figure 9a and 9b. Figure 9a and b show a simplified field area river right bank geology (a) and a cross section of the slope with all the units, their relative thickness and location, location and density of seeps, and probable locations of failure planes (b).

Unit A1 extents from the surface (210 feet above sea level) to about 130 feet above sea level, where the confining layer, layer C1, begins. During field reconnaissance the 80 foot thick A1 unit was identified as a loose to medium dense sand and gravel. The C1 layer was identified as bedded, matrix supported, glacial till containing a large percentage of cobbles (about 45 percent). From the subsurface SPT it was discovered that the recessional outwash, unit A1, had cohesion values ranging from 50 – 62 kPa, an angle of internal friction of about 38 degrees, and based on the corrected N values this unit can be described as a dense unit (Shannon and Wilson, 1997; Aspect, 2017). The same test showed that the underlying 30-foot-thick glacial till layer, unit C1, had a cohesion value ranging from 500 – 600 kPa, and angle of internal friction of about 52 degrees, and the corrected N values identify this layer as a dense unit (Shannon & Wilson, 1997; Aspect, 2017). Blows per foot and corrected N values for these two units can be found on Table 3 under the A1 and C1 units.

Unit A2 extends from the bottom of unit C1 (about 100 feet above sea level) to about 65 feet above sea level. The 35-foot-thick Pre-Vashon non-glacial unit was identified as a dry, very dense coarse-grained sand that has been disturbed by roots and burrowing wildlife and thus has a 3.5-foot-thick loose/weakened layer covering it. Unit A2 is crudely bedded, consisting of primarily sand with subrounded to subanglular grains and few cobbles. Due to the presence of a relatively high percentage of red andesite grains and the presence of large yellow micas, the underlying C2 unit was identified as an interglacial layer. Unit C2 was oxidized and contained dark grains that made up a gravely, silty, fine sandy unit, while Unit A2 was only slightly oxidized. Though the thickness of the layer is currently unknown, this same C2 unit was found at a higher elevation upriver in the tributary at the western end of the field area. This observation

lead me to the assumption that the units are dipping slightly to the east-southeast. Unit C2 had a larger concentration of silt that Unit A2. From the subsurface SPT it was discovered that the A2 unit has a cohesion value ranging from 195-220 kPa, an angle of internal friction of about 31 degrees, and the corrected N units describe this unit as a very dense unit (Shannon & Wilson, 1997; Aspect, 2017). The same test showed that the underlying C2 unit has a cohesion value ranging from 700 – 800 kPa, and angle of internal friction of about 53 degrees, and based on the corrected N values can be characterized as a very dense material (Shannon & Wilson, 1997; Aspect; 2017). Blows per foot and corrected N values for these two units can be found on Table 3 under the A2 and C2 units.

Landslide Inventory Results and Field Area Factor of Safety

As mentioned before, the current landslide inventory of Pierce County does not include the large complex rotational landslide deposit located to the east of the field area or any of the small landslide deposits visible on lidar delineated in Figure 4. Using the same method described in Slaughter et al., (2017), I mapped and analyzed all of the obvious landslides. I delineated four landslide scarps and at least eight landslide deposits in the field area (Figure 4 and Table 4). From the lidar imagery and the results from Table 4, it would seem that, based on their size, all of the deposits originate from deep-seated landslide events.

Since it was the largest, the results of my analysis for the large landslide complex (landslide ID – 1, Figure 4) on the eastern edge of the field area is presented in this paragraph. By following the steps outlined in Slaughter et al. (2017) it was discovered that the average local slope around the large landslide to the east is about 68 degrees. The large eastern landslide area has been heavily reworked by humans. The headscarp is about 60 feet in height. Using the equation in Slaughter et al. (2017), it was determined that the failure depth of the complex landslide is about 60 feet. The landslide covers an area of 350,000 square feet and has a volume about 21,000,000 cubic feet.

After accounting for the 4 degree south-east dip, which can offset the unit heights by about 105 feet on the eastern edge of the field area, and by shifting each unit height up 3.5 meters every 50 meters during calculations, a factor of safety assessment of the field area was completed. In order to get the best range of data a summer and winter calculation was conducted on both of the susceptible contacts in the shallow factor of safety calculations. In this Capstone project, the summer scenario correlates with a model with all components set to produce a stable slope situation (high cohesion, low wetness factor, and low local slope), while a winter scenario correlates with a model with all components set to produce a landslide (low cohesion, high wetness factor, and high local slope). In these calculations the summer A1-C1 scenario has an *m* value of 40% while the winter A1-C1 scenario *m* value is 80%, and the summer A2-C2 scenario has an *m* value of 60% and the winter A2-C2 scenario *m* value is 90%. From the field site factor of safety tables (Tables 5a and b) we can see that the majority of the field area is well below 1 for shallow landsliding and the A2 unit is below or close to 1 for deep sliding, which means that

these slopes are at risk of experiencing both a shallow and deep failure. At point 9 (middle of the field area, about where the small depression in the slope is) the C1 unit reaches or lies just underneath the terrace surface at the top of the upland and the top of the C1 unit was no longer considered a possible susceptible geologic contact for both the deep and shallow landslides. At this point the factor of safety equation was modified to account for the new cohesion value and new angle of internal friction derived from unit A2. At point 11, approximately where the western protrusion begins to form on the east side, the C2 unit reached the surface, however, since the thickness is unknown, the unit was assumed to continue throughout the western portion of the field area. Once again, the factor of safety equation was modified to account for the C2 units cohesion value and new angle of internal friction. The final results of the factor of safety models are area displayed in Figures 10 – 15.

Since the same factor of safety intervals were used for all the factor of safety model legends, areas at risk of failure can be identified. We can see from the shallow-seated A1-C1 contact models (Figures 10 and 11) that the area at the greatest risk of failing along this contact boundary is on the western face of the existing landslide and on the concave face that runs parallel to the valley. From these two figures we can also see that the most stable section is where the C1 unit reaches the terrace surface at the top of the upland. We can see from the shallow-seated A2-C2 models (Figures 12 and 13) that the area most likely to experience a shallow landslide along this contact boundary are on the convex face that runs parallel to the valley. Likewise, these two figures reveal that the most stable section along the surface is on the western edge of the field area, where the C2 unit reaches the surface. Figure 14 reveals that a deep-seated landslide is unlikely to occur along the A1-C1 susceptible geologic contact. Figure 15 shows that the areas at the greatest risk of a deep landslide along the A2-C2 contact are also on the two faces that run parallel to the valley, and that where the C2 unit reaches the surface is the area least likely to fail along this susceptible geologic contact.

Discussions

Field Area Property Susceptibility Analysis

By combining the observations and results from the various tests and models, an shallow and deep landsliding model was created. These models delineated specific areas along the field area that were at a higher or lower risk of experiencing a shallow or deep landslide event based on the findings and calculations performed in this study.

To create the final deep-seated landslide risk model the factor of safety model results, which took into account the local slope of the native units, were combined with proximity to existing and mapped landslide scarp. The result of this combination is the model displayed in Figure 16. This final model showed that the areas at the greatest risk of deep-seated landsliding

are those closest to the large eastern landslide and those slopes that have faces that run parallel to the valley. Due to the 4 degree east-southeast dip of the geologic units, the residential properties located close to the western section of the large eastern landslide are at the greatest risk of sliding. According to the data, the area at lowest risk of deep landsliding is located on the western edge of the field area. This is most likely due to the fact that the very dense C2 unit underlying the area. However, the area between where the C1 and C2 units reach the surface is at risk of experiencing a deep-seated landslide

To create the shallow landslide risk model the surface SPT N values, NDVI results, local slope, and field observations were combined into a multivariable calculation and then simplified to show the results more clearly. This model is displayed in Figure 17. Here we see that the area's most at risk of shallow landsliding are located in the middle of the field area (on the convex face that runs parallel to the valley) and, to a lesser degree, the concave face to the east that runs parallel to the valley. This is most likely due to the fact that a thin (a few feet thick) colluvial layer covers these parts of the field area. According to the shallow-landslide risk model, three areas are relatively safe from experiencing a shallow landslide. Two of those locations are where the C1 and C2 units reach the top of the terrace (the green areas in the middle and on the western edge of the field area). Since theses layers are denser and harder than their overlying counterparts, these two regions are displayed as more stable and less likely to result in surface failure. Surprisingly, the data also shows that the western face of the large eastern landslide is relatively safe from shallow landsliding. This is most likely due to the dense evergreen population on this face and the fact that this face has an average slope of about 35 degrees, and the angle of internal friction of the colluvial unit is about 38 degrees. In addition, the colluvium may have even been thinner here that elsewhere.

Conclusion

The ultimate goal of this Capstone Project was to create a deep and shallow landslide susceptibility model of a segment of the right bank of Chambers Creek Basin. Using a combination of field and GIS analysis, along with the appropriate values of material strength, susceptible geologic contacts were determined and used as input variables in factor of safety analyses. In order to make the factor of safety models as representative of the local geology as possible, calculations were done on both susceptible geologic contacts (identified based on seepage zones). These factor of safety models were then combined with slope, curvature, vegetation, and field observations to create a landslide hazard model. The results of this combination of data are presented in the deep (Figure 16) and shallow (Figure 17) seated landslide risk models. According to the data, the highest risk of shallow landsliding is located in the center of the field area, between where the Pre-Vashon till (C1) and the coarse grained Pre-Vashon non-glacial deposit (C2) units reach the surface. The highest risk of deep landsliding is located on the eastern extent of the field area, where a concave, protruding section sticks out into

the valley (between the western face of the large eastern landslide complex and where the C1 unit reaches the surface). Both models agreed that the lowest risk of both deep and shallow landsliding is located on the western edge of the field area, most likely due to the strength of the underlying C2 unit. In addition, from this Capstone project I learned that there are at least eight landslide deposits (most likely of deep-seated origin) and at least four headscarps in just this small field area along the river right bank of Chambers Creek. Finally, the surface SPT data collected may be indicating the age of the landslide events in this area.

References

Aspect Consulting, 2017, Field description reference guide according to ASTM D 2488, Personal communication.

Borden, R.K. and Troost, K.G., 2001, Late Pleistocene Stratigraphy in the South-Central Puget Lowland, Pierce County, Washington, Washington State Department of Natural Resources, Report of Investigations 33, pg. 40.

Bretz, H.J., 1910, Glacial lakes of Puget Sound, The Journal of Geology, Vol. 18, No. 5, pg. 448-458.

Brown and Caldwell, 1985, Clover/Chambers Creek geohydrologic study for Tacoma-Pierce County Health Department: Seattle, WA., pg. 1-75.

Burns, W. J., Madin, I. P., 2009, Protocol for inventory mapping of landslide deposits from light detection and ranging (LIDAR) imagery: Oregon Department of Geology and Mineral Industries, Special Paper 42, pg. 30.

Fleming, R.W., Johnson, A.M., 1994, Landsliding in Colluvium, U.S. Geologic Survey Bulletin, 2059-B, p.g. 1-123.

GIS Geography, What is NDVI (Normalized Vegetation Index?), Accessed August 2018, https://gisgeography.com/ndvi-normalized-difference-vegetation-index.

GIS Image: NAIP2013, Imagery Services, ArcMap View, http://wagda.lib.washington.edu:6080/arcgis/rest/services/Imagery_services/NAIP2013/ImageServer, Accessed February 2018.

Laprade, W., 2017, Shannon & Wilson, Personal communication.

Menashe, E., 1983, Vegetation Management: A Guide for Puget Sound Bluff Property Owners, Shorelands and Environmental Assistance Program, Washington Department of Ecology, pg. 1-54.

Mickelson K.A., Jacobacci, K.E., Contreras, T.A., Biel, A., and Slaughter, S. L., 2017, Landslide inventory, susceptibility, and exposure analysis of Pierce County, Washington, Washington State Department of Natural Resources, WSGS, Report of Investigation 39, pg. 1-35.

Myers, R.D., 1993, Slope Stabilization and Erosion Control Using Vegetation: A Manual of Practice for Coastal Property Owners, Shorelands and Coastal Zone Management Program, Washington Department of Ecology, Publication 93-30, pg. 1-23.

Pierce County Public Works and Utilities, 2010, Section 3 – Physical and Environmental Inventory, Sewer Utility: Unified Sewer Plan Update, https://www.co.pierce.wa.us/DocumentCenter/View/1093.

Rodgers, David J., 2006, Subsurface exploration using the standard penetration test and cone penetomerter test, Environmental and engineering geosciences, pg. 1-32.

Savoca, M.E., Welch, W.B., Johnson, K.H., Lane, R.C., Clothier, B.G., and Fasser, E.T., 2010, Hydrogeologic framework, groundwater movement, and water budget in the Chambers-Clover Creek Watershed and vicinity, Pierce County, Washington, U.S. Geological Survey Scientific Investigations Report 2010–5055, pg. 1-58.

Shannon & Wilson, 1997, Field characterization reference guide according to ASTM D 2487, Personal communication.

Slaughter, S. L., Burns, W.J., Mickelson K.A., Jacobacci, K.E., Beil, A., Contreras, T.A., 2017, Protocol for landslide inventory mapping from lidar data in Washington State, Washington State Department of Natural Resources, WGS, Bulletin 82, pg. 1-23.

Troost, K.G., 2007, Jokulhlaups from glacial lake Puyallup, Pierce County, Washington, Geological Society of America, Cordilleran Section Meeting, Bellingham, WA, Abstracts with Programs, Vol. 39, no. 4, pg. 13.

Troost K.G. and Booth D.B., 2008, Geology of Seattle and the Seattle area, Washington, The Geologic Society of America, Issue XX, pg. 1-35.

Troost, K.G., Booth, D.B., and Borden, R.K., in press, Geologic map of the Steilacoom 7.5-minute quadrangle, Washington: U.S. Geological Survey Scientific Investigations Map, scale 1:24,000.

USGS Stream Gauge System, Chambers Creek below Leach Creek near Steilacoom (gauge 12091500).

Utili, S. and Nova, R., 2007, On the optimal profile of a slope, Soils and Foundations, Vol. 47(4), pg. 717-729.

Washington State Department of Natural Resources: Division of Geology and Natural Resources; Pierce 2011 Lidar Data; Last updated 2011; http://lidarportal.dnr.wa.gov/#47.19974:-122.50408:12, Accessed January 2018.

Figures and Tables

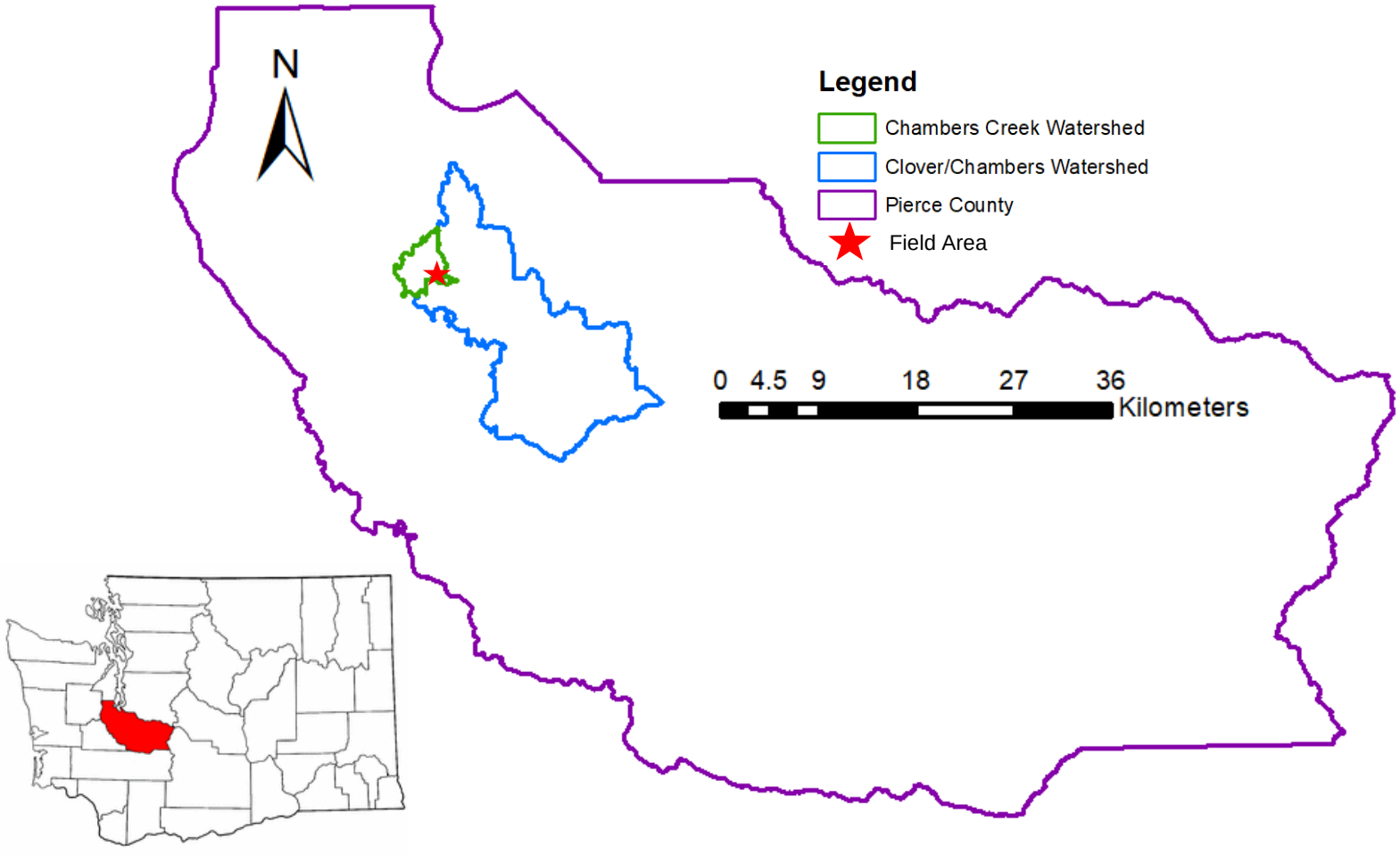

Figure 1: Location Map. Location of the field area (red star). On the bottom left is a map showing the various counties in Washington with Pierce County highlighted in red.

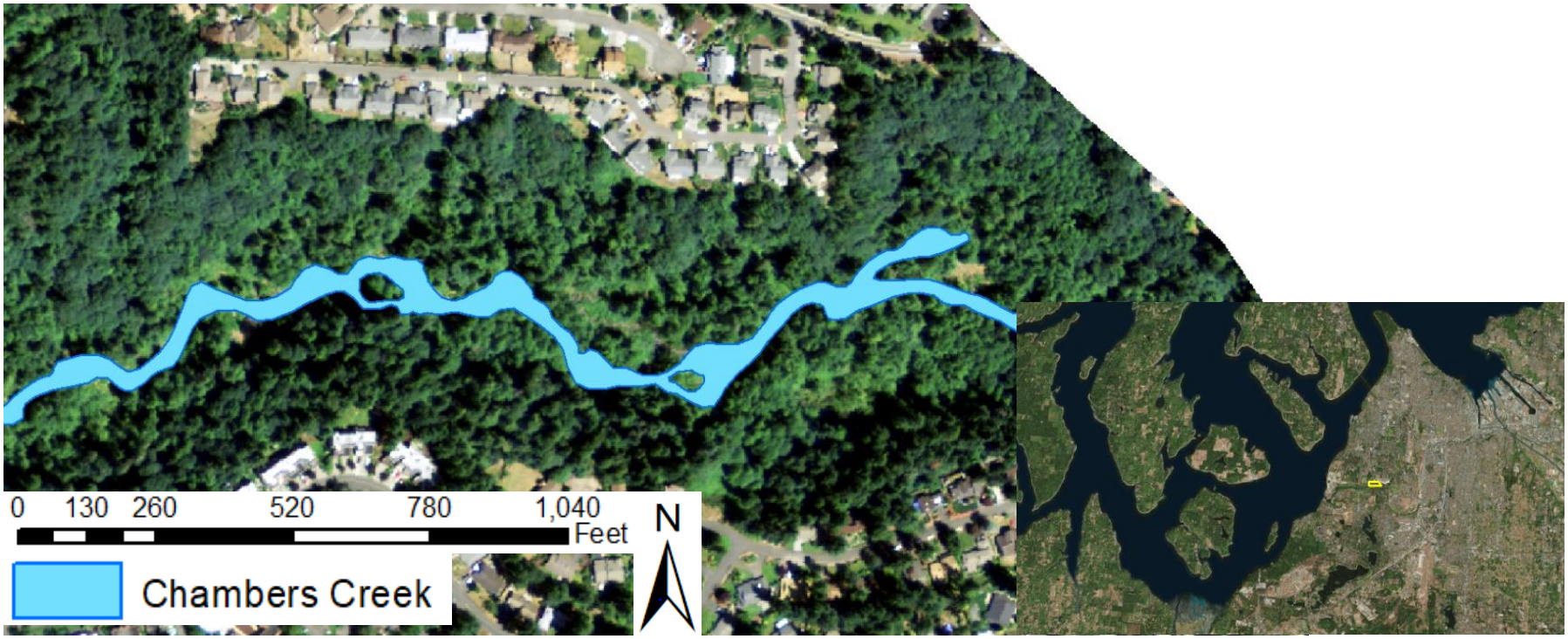

Figure 2: Field Area. Location of the field area (yellow polygon) relative to the southern extent of Puget Sound (bottom right image). The main image shows the neighborhood located directly to the north (above) of the field area (right bank of Chambers Creek Basin).

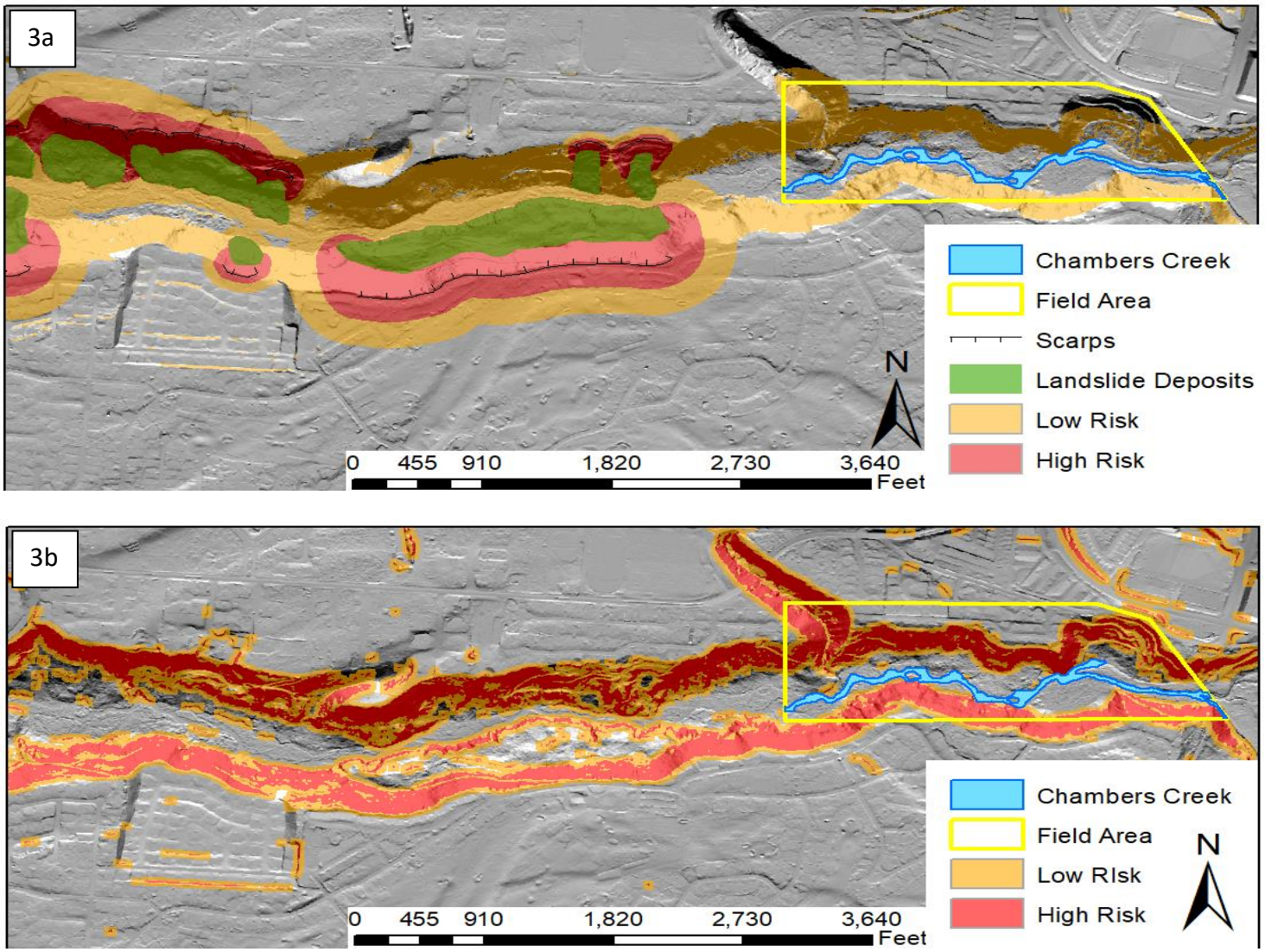

Figures 3 a and b: Pierce County Deep (a) and Shallow (b) Seated Landslide Risk maps of the Chambers Creek Basin (Mickelson et al., 2017). The field area is marked by the yellow polygon. Chambers Creek is only delineated within the study area.

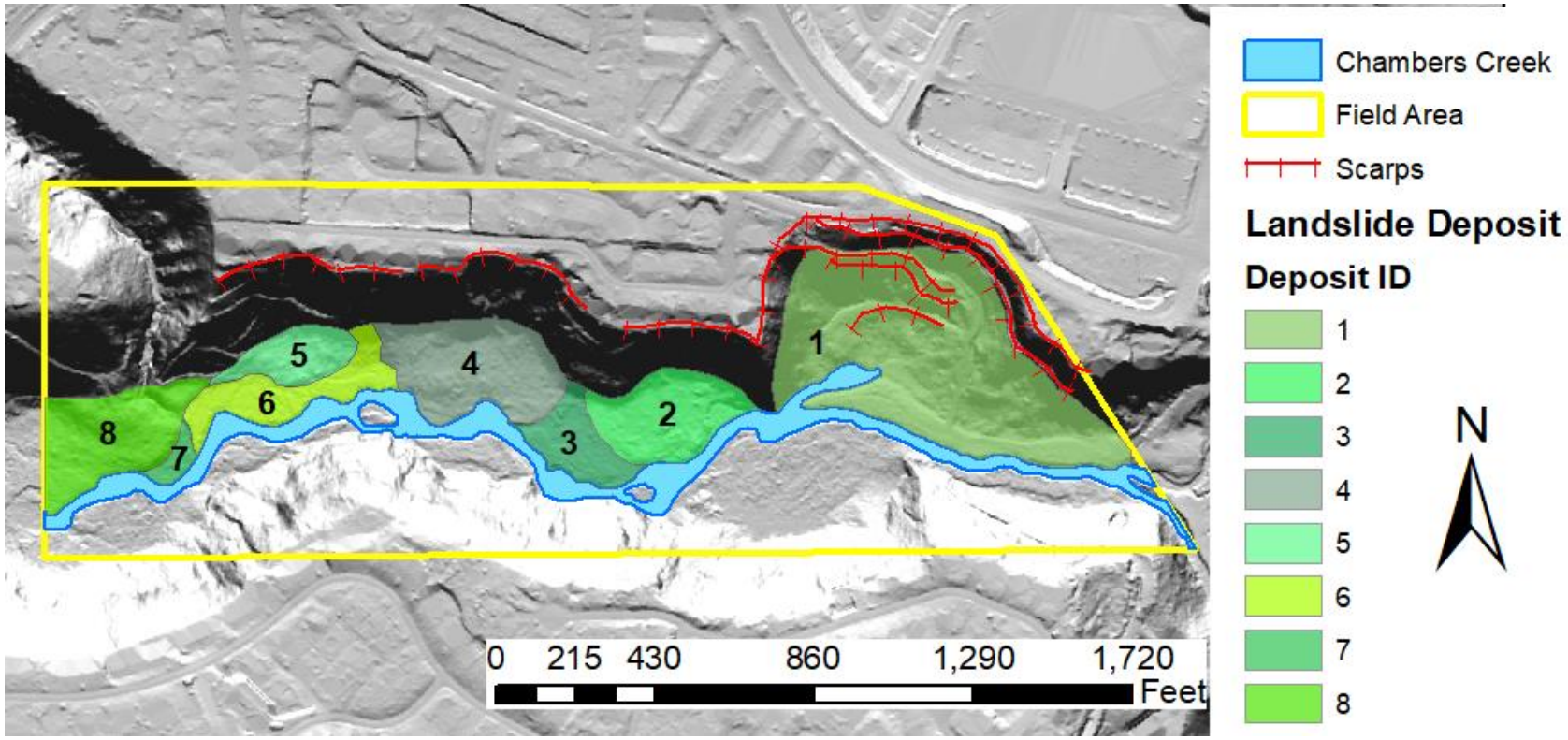

Figure 4: Landslide Inventory of field area. Landslide scarps are delineated in red hash-marked line. Landslide deposits are the various shades of green.

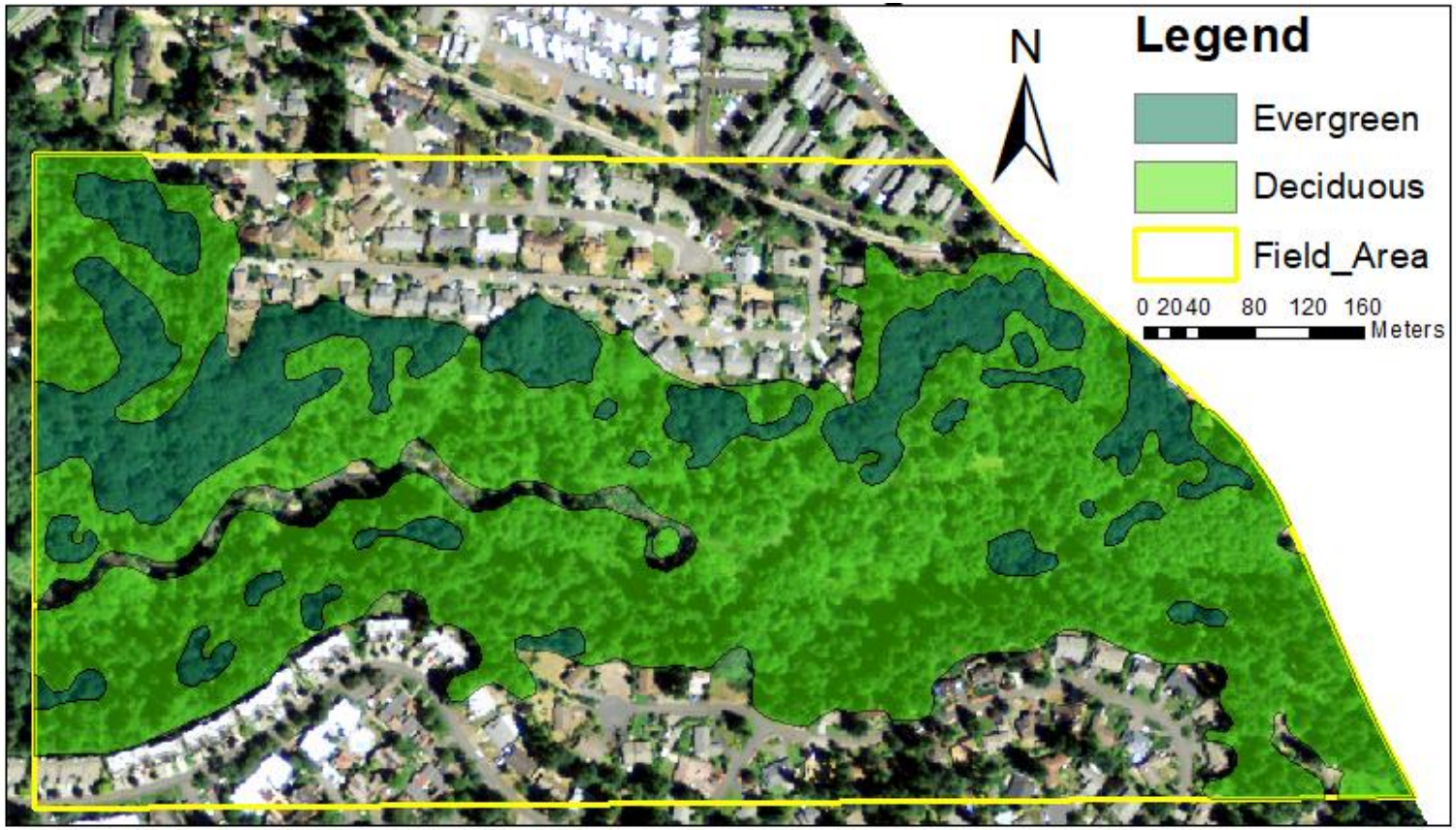

Figure 5: Chambers Creek Vegetation. Image showing vegetation distribution in the field area, obtained from the NDVI. Areas of predominantly evergreen trees are indicated with the dark green polygons while areas with predominantly deciduous trees are shown in light green.

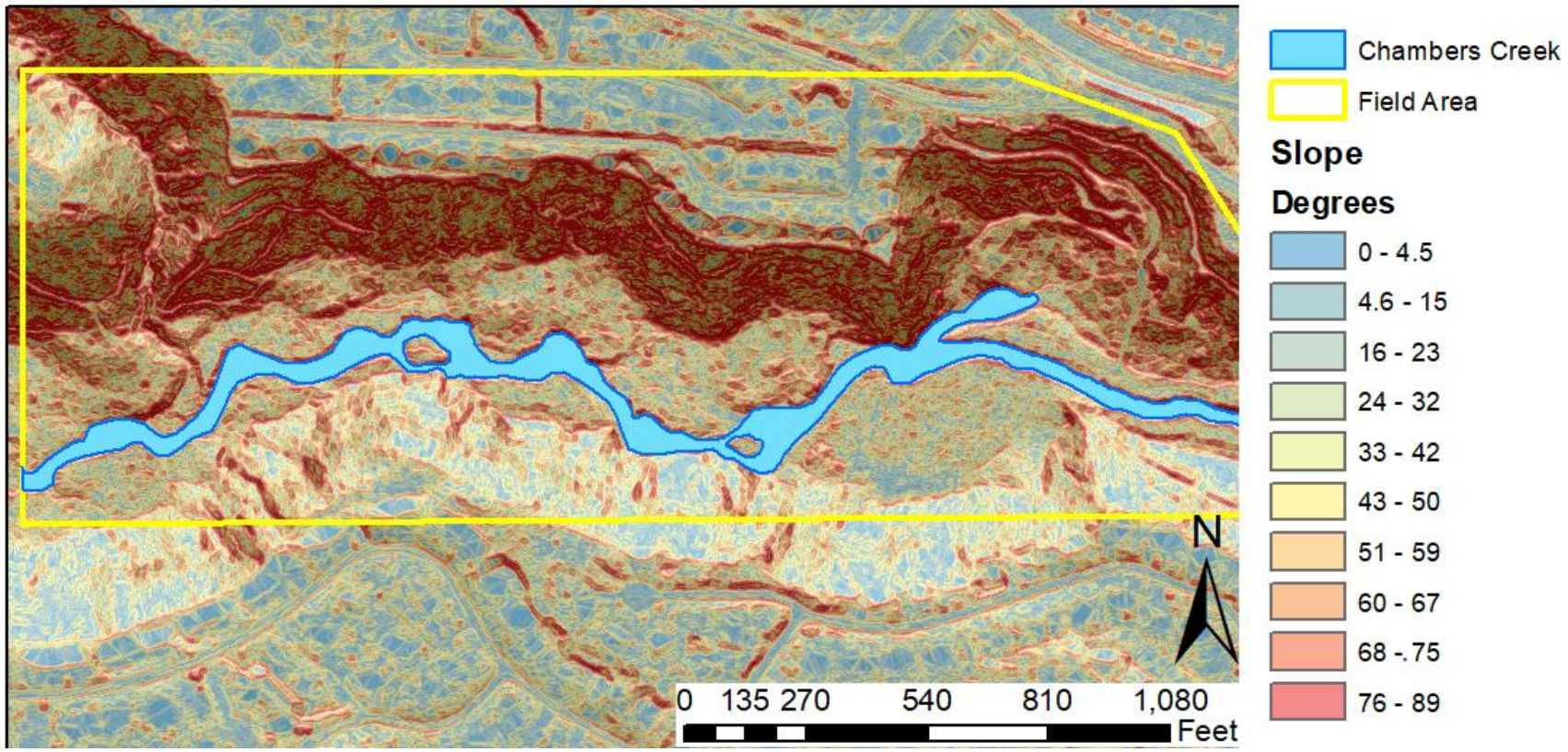

Figure 6: Field area slope in degrees. Calculated from the 2011 lidar image. Right bank (north) slopes range from 50 to 80 degrees. Left bank (south) slopes range from 30 to 50 degrees.

Chambers Creek Colluvial SPT Data		
Site	Blows/ft	Corrected N Value
1	37	4.32
2	40	4.67
3	28	3.27
4	26	3.04
5	23	2.69
6	34	3.97
7	38	4.44
8	45	5.26
9	40	4.67
10	42	4.91
11	44	5.14
12	42	4.91
13	39	4.56
14	33	3.86
15	16	2.25
16	23	3.23
17	8	1.12
18	14	1.97
19	18	2.53
20	20	2.81
21	22	3.09
22	26	3.66
23	39	5.48
24	13	1.83
25	18	2.53
26	10	1.41
27	21	2.95
28	26	3.66
29	30	4.22
30	29	4.08
31	14	1.97
32	22	3.09
33	18	2.53
34	27	3.80
35	33	4.64
36	34	4.78

Range	
Cohesion (kPa)	12-25
Angle of Internal Friction (degrees)	27-32
Density	Loose

Table 1: Table indicating surface colluvium SPT corrected N values and correlated cohesion, angle of internal friction, and density.

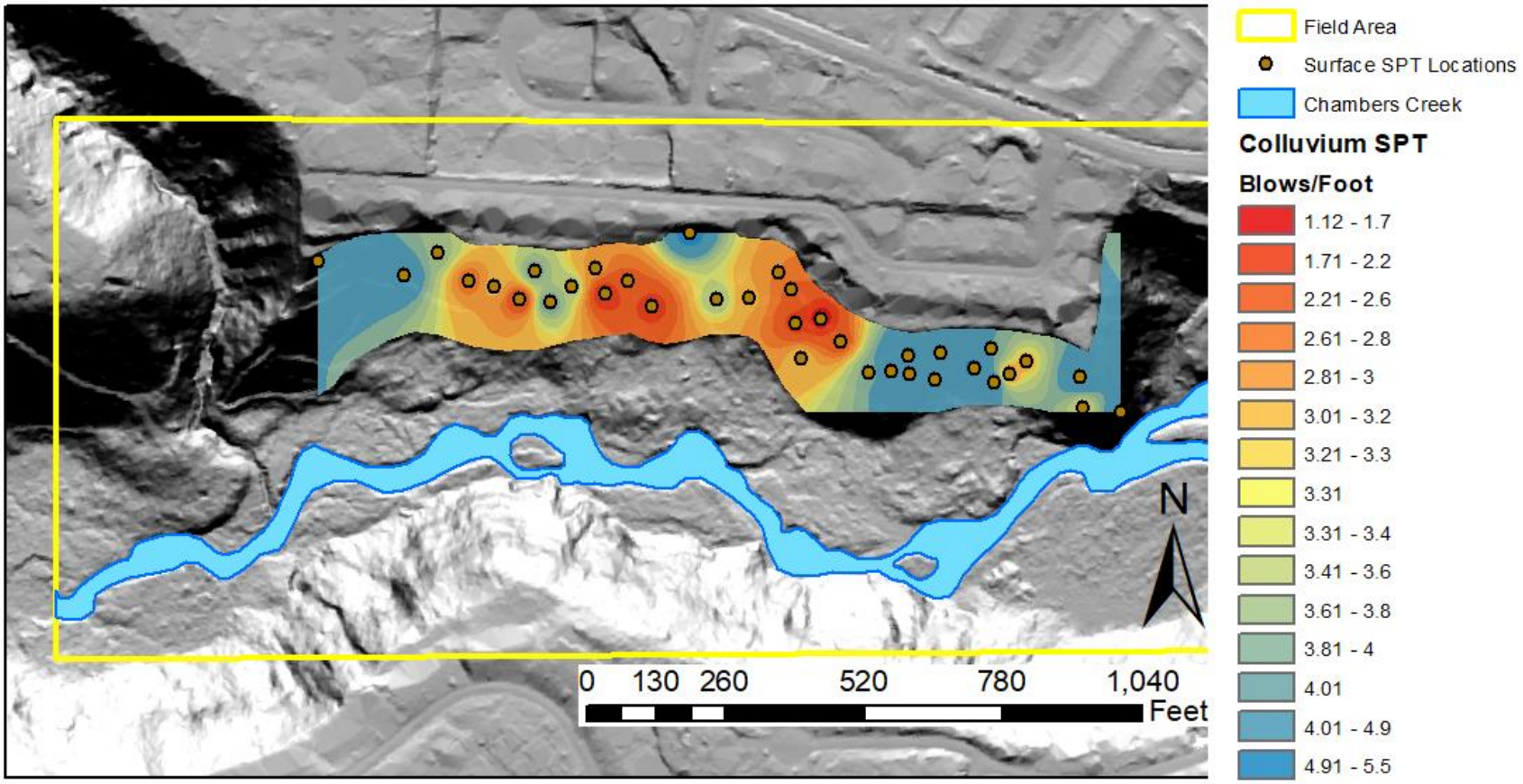

Figure 7: Image displaying surface SPT blows/foot value data and locations of test sites.

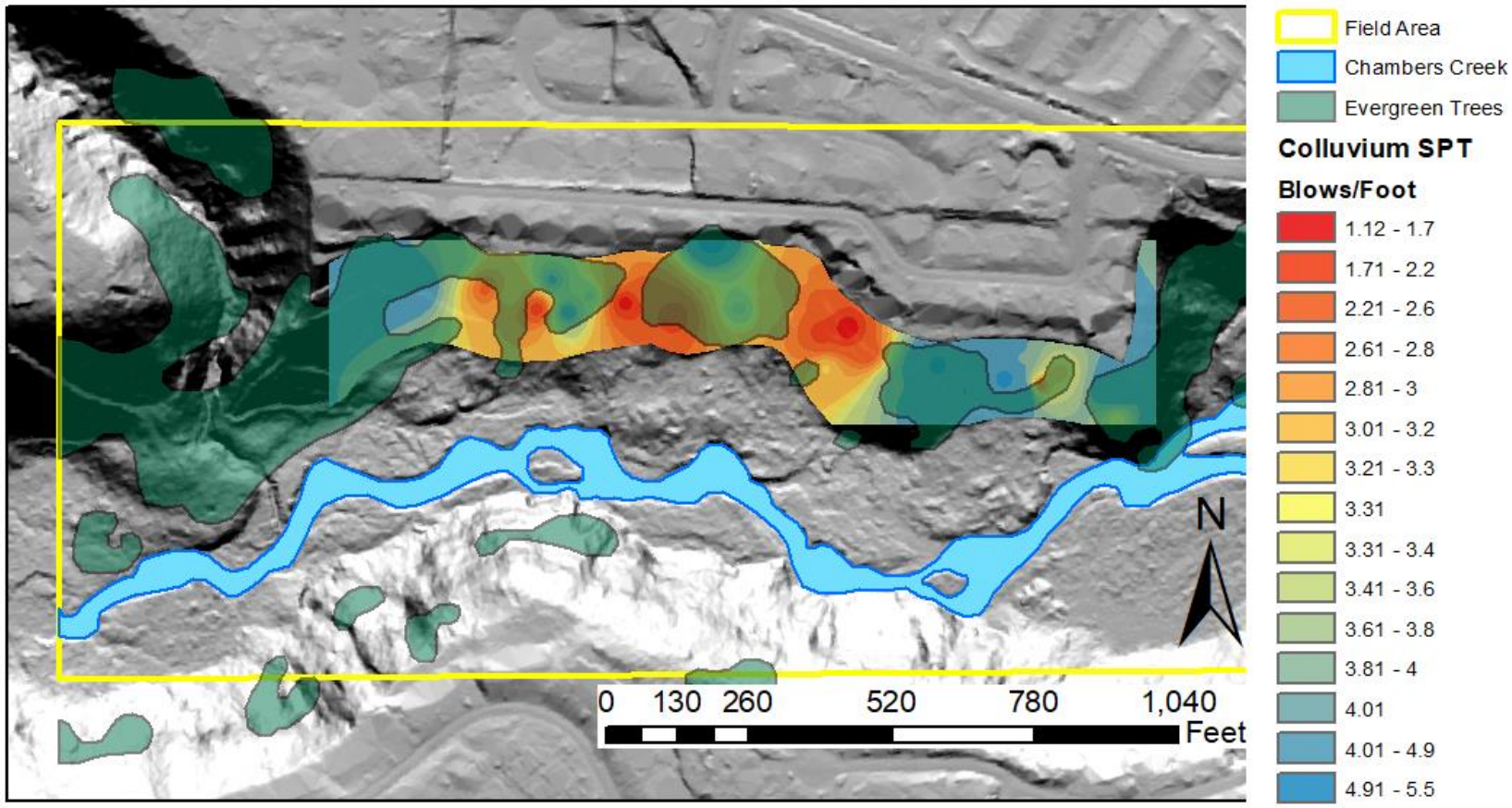

Figure 8: Combined SPT blows/foot and NDVI data for right bank of Chambers Creek Basin.

Field Site Geologic Units					
Unit Name	Unit Abbreviation	Unit Title in Report	Unit Description	Ave. C (kPa)	Ave. ϕ (°)
Colluvium	Qmw	z	Mixture of artificial fill near the top of the slope, and material eroded from the Vashon and Pre-Vashon units further downslope. This unit was very loose to loose and was primarily a mixture of sand and gravel with few cobbles with variable silt content. Dry to moist.	18	30
Vashon Recessional Outwash	Qvr	A1	Loose to medium dense alternating layers of stratified sand and gravel with moderate to well sorting. Dry to saturated with depth. Jökulhlaup deposits.	56	28
Pre-Vashon Till	Qpogt	C1	Bedded, matrix supported diamict with sub-angular to rounded clasts containing a large percentage of cobbles (about 45 percent). Perches groundwater.	350	45
Pre-Vashon Non-Glacial Coarse-Grained Unit	$Qpon_c$	A2	Dense coarse grained sand, crudely bedded, with subrounded to subanglular grains and few cobbles. Slightly oxidized in some places. Variably dry to saturated grains and few cobbles.	190	31
Pre-Vashon Non-Glacial Fine-Grained Unit	$Qpon_f$	C2	Very dense silty sand to sandy silt with some oxidized finer-grained interbeds. Presence of red andesite clasts, organic matter, and yellow mica identify unit as interglacial deposit. Moist to saturated in some layer. Perches groundwater.	550	53

Table 2: Field Site Geologic Units. Unit description and nomenclature along with average cohesion (C) and angle of internal friction (ϕ).

9a

West

Kobayashi Park

East

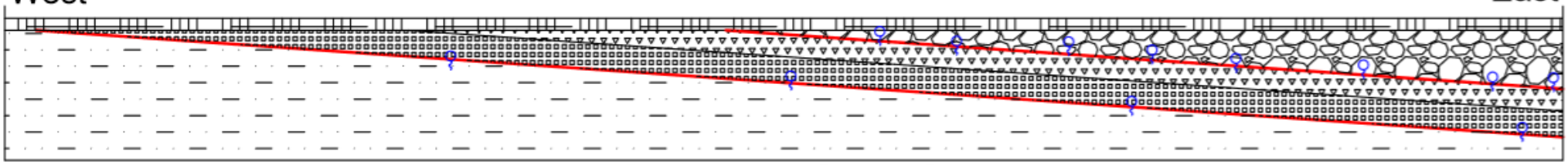

Artificial Fill

Vashon Recessional Outwash (A1)

Pre-Vashon Till (C1)

Pre-Vashon Non-Glacial Coarse-Grained Unit (A2)

Pre-Vashon Non-Glacial Fine-Grained Unit (C2)

Susceptible Geologic Contact

Seeps

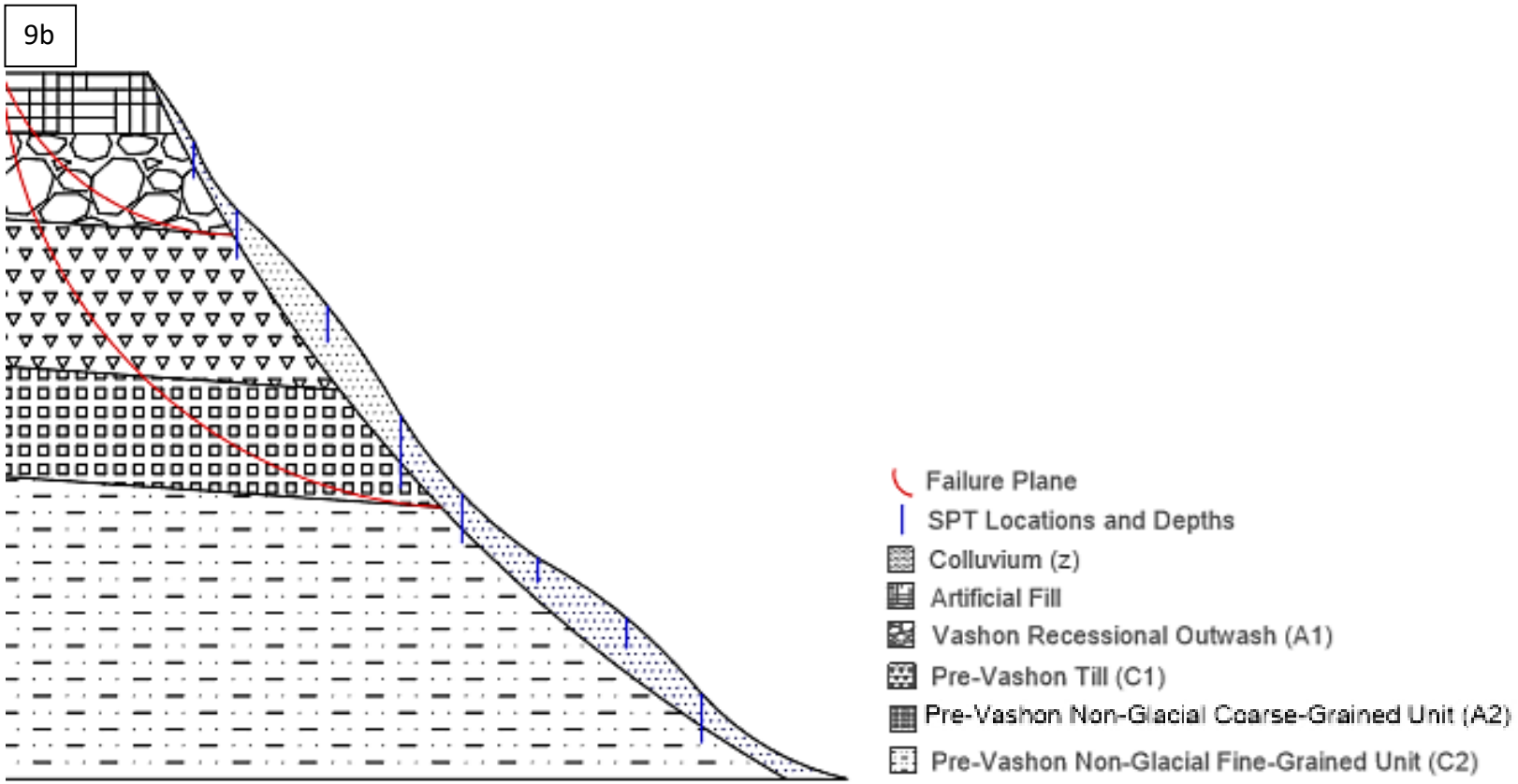

Figures 9a and b: Figure 9a (top) displays a simplified version of the geology of the river right bank within the field area as seen from the river. Table 4b displays a cross section of the field area's slope, with the colluvium layer, SPT locations and depths, and the two possible failure planes.

Chambers Creek Subsurface SPT Data					
Test	Blows/ft	Corrected N Value		Values	
Vashon recessional outwash (A1)					
4	96	11.22		**C (kPa)**	50 - 62
5	88	10.28		**AoIF (°)**	30
6	103	12.03		**Density**	Dense
Pre-Vashon Till (C1)					
1	413	48.25		**C (kPa)**	300 - 400
2	431	50.35		**AoIF (°)**	45
3	392	45.80		**Density**	Dense
Pre-Vashon course-grained non-glacial (A2)					
10	250	29.21		**C (kPa)**	175 - 200
11	278	32.48		**AoIF (°)**	34
12	269	31.43		**Density**	Very Dense
Pre-Vashon fine-grained non-glacial (C2)					
7	924	107.95		**C (kPa)**	500 - 600
8	906	105.85		**AoIF (°)**	53
9	1005	117.42		**Density**	Very Dense

Table 3: Table indicating subsurface SPT corrected N values for the subsurface units along with correlated Cohesion (C), Angle of internal friction (AoIF), and Consistency (Con).

Field Area Landslide Inventory					
Landslide ID	Ave. Slope (°)	Headscarp Height (ft)	Failure depth (ft)	Area Cover(ft^2)	Volume (ft^3)
1	68	60	60.0	350,000	21,000,000
2	65	28	11.8	81,500	964,857
3	70	45	15.4	47,000	723,831
4	61	55	26.7	112,000	2,987,509
5	63	27	12.3	38,000	465,984
6	64	48	21.1	100,000	2,105,091
7	66	-	-	10,000	-
8	58	46	24.4	92,000	2,243,304

Table 4: Field site landslide inventory. Inventory containing landslide characteristics for all landslides in field area starting from west to east.

Field Site Shallow Factor of Safety						
	Local Slope		A1-C1 contact		A2-C2 contact	
Point	Low	High	Low	High	Low	High
1	50	65	0.82	0.39	0.75	0.52
2	55	70	0.75	0.43	0.52	0.48
3	60	70	0.63	0.45	0.48	0.47
4	65	75	0.44	0.22	0.41	0.38
5	65	80	0.49	0.55	0.38	0.4
6	55	70	0.59	0.61	0.55	0.47
7	60	70	0.33	0.88	0.42	0.49
8	40	80	1.6	2.3	0.98	0.52
9	65	75	-	-	0.52	0.5
10	60	75	-	-	0.38	0.46
11	60	70	-	-	0.46	0.58
12	45	60	-	-	1.1	0.82
13	55	70	-	-	1.5	0.77
14	55	70	-	-	1.6	0.79

Field Site Average Deep Factor of Safety			
Point	Local Slope	A1-C1	A2-C2
1	59	1.31	1
2	65	1.28	0.89
3	67	1.35	0.83
4	69	1.38	0.74
5	74	1.5	0.67
6	64	1.26	0.9
7	66	1.3	0.83
8	60	1.29	0.95
9	71	-	0.68
10	68	-	0.73
11	67	-	0.84
12	50	-	1.4
13	58	-	0.98
14	57	-	1.2

Tables 5a and b: Table 5a (left) displays Factor of Safety calculations for four shallow landslide scenarios for the A1-C1 and A2-C2 contacts (A1-C1 Low, A1-C1 High, A2-C2 Low, and A2-C2 High), along with the range of local slope values every 160 feet along the field area from east to west. Table 5b displays Factor of Safety measurements for the A1-C1 and A2-C2 contacts for a deep landslide scenario.

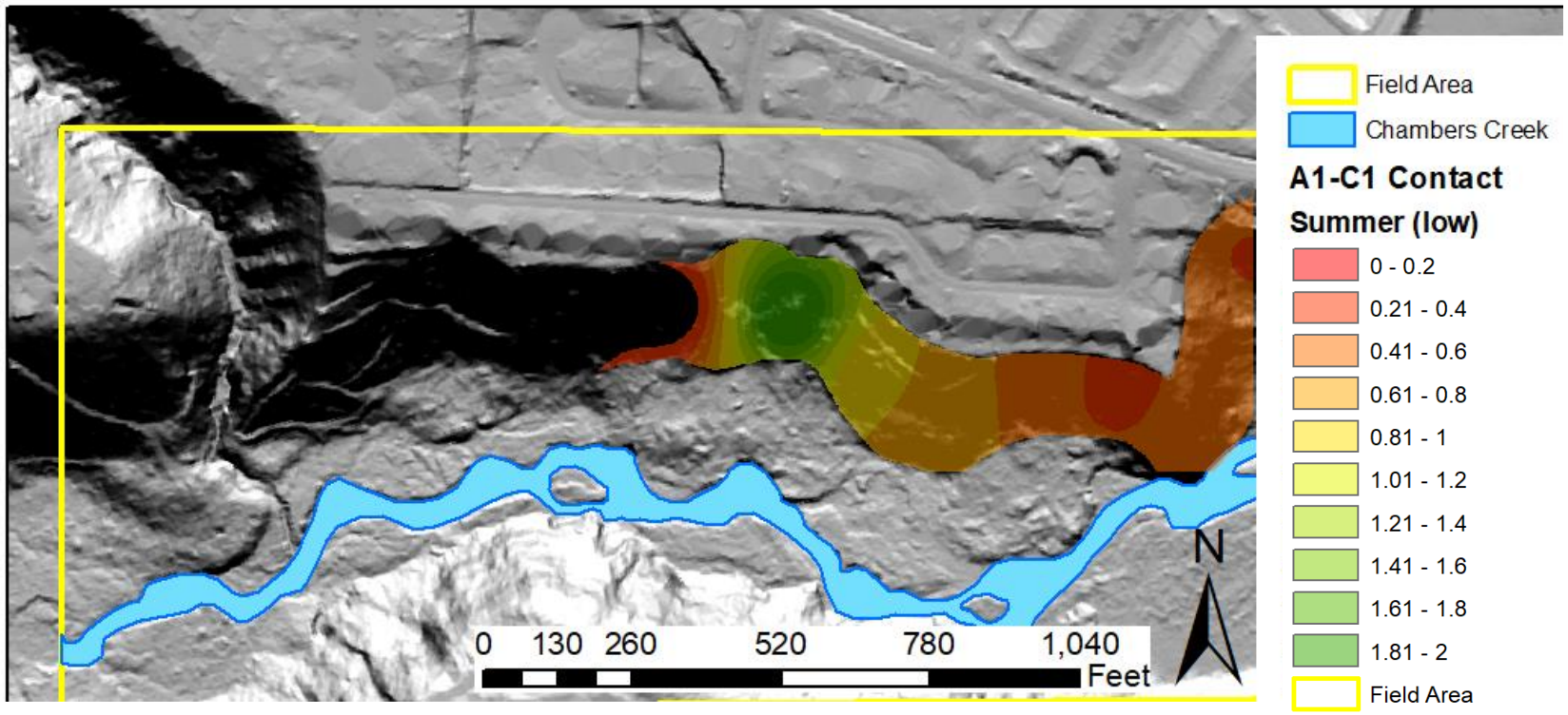

Figure 10: Field area shallow-seated Factor of Safety Model for low scenario (summer flow) along the A1-C1 contact. Since this model is based on a landslide failure occurring on the A1-C1 susceptible geologic contact, the data ends where the contact reaches the top of the terrace.

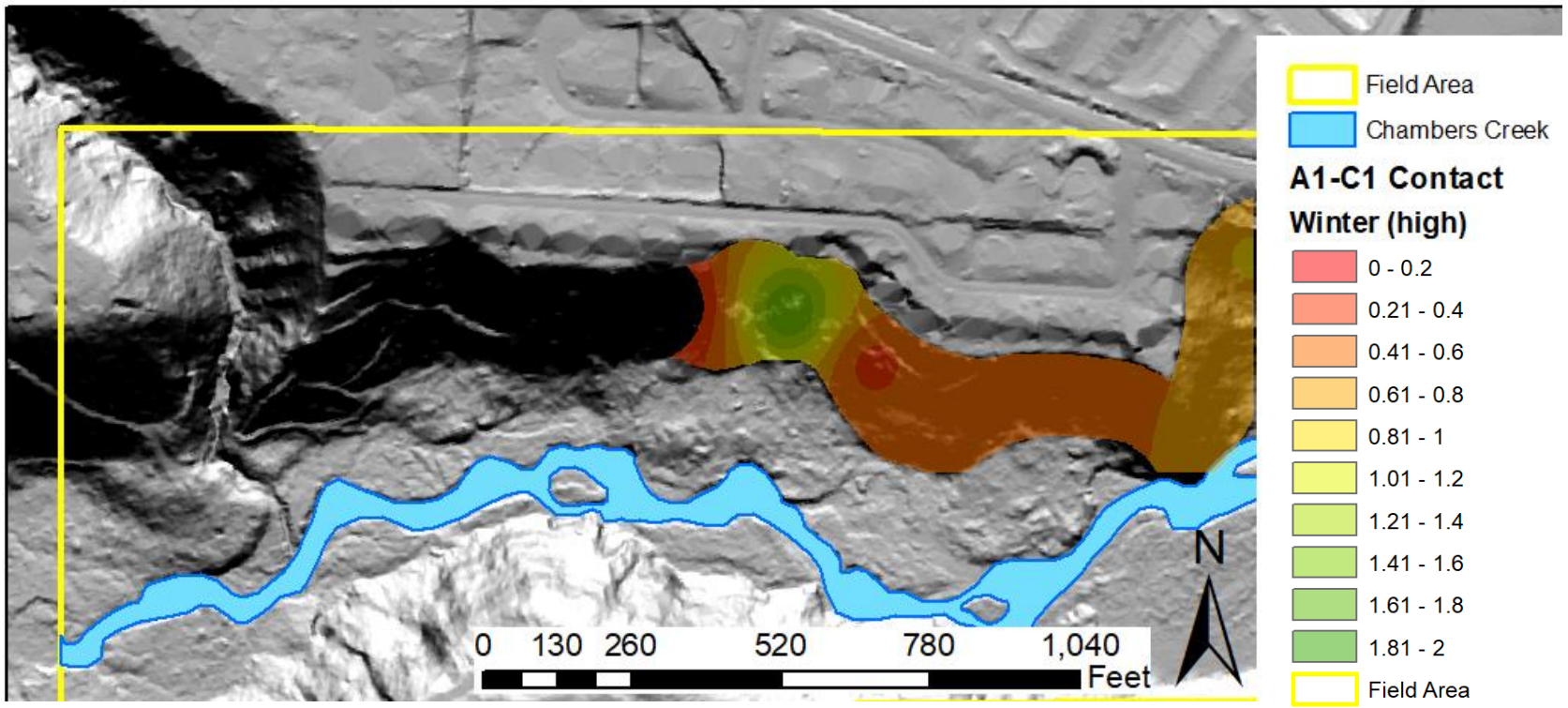

Figure 11: Field area shallow-seated Factor of Safety Model for high scenario (winter flow) along the A1-C1 contact. Since this model is based on a landslide failure occurring on the A1-C1 susceptible geologic contact, the data ends where the contact reaches the top of the terrace.

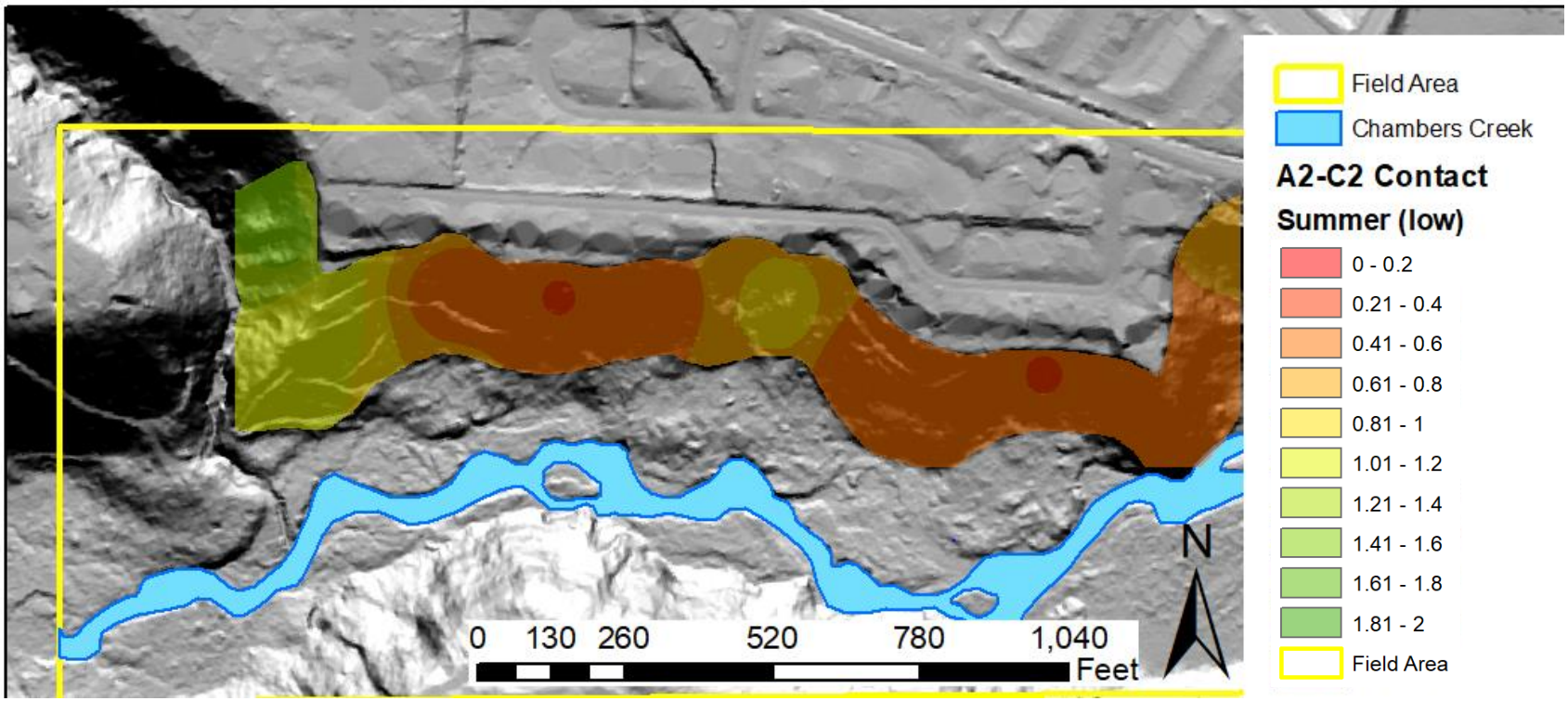

Figure 12: Field area shallow-seated Factor of Safety Model for low scenario (summer flow) along the A2-C2 contact.

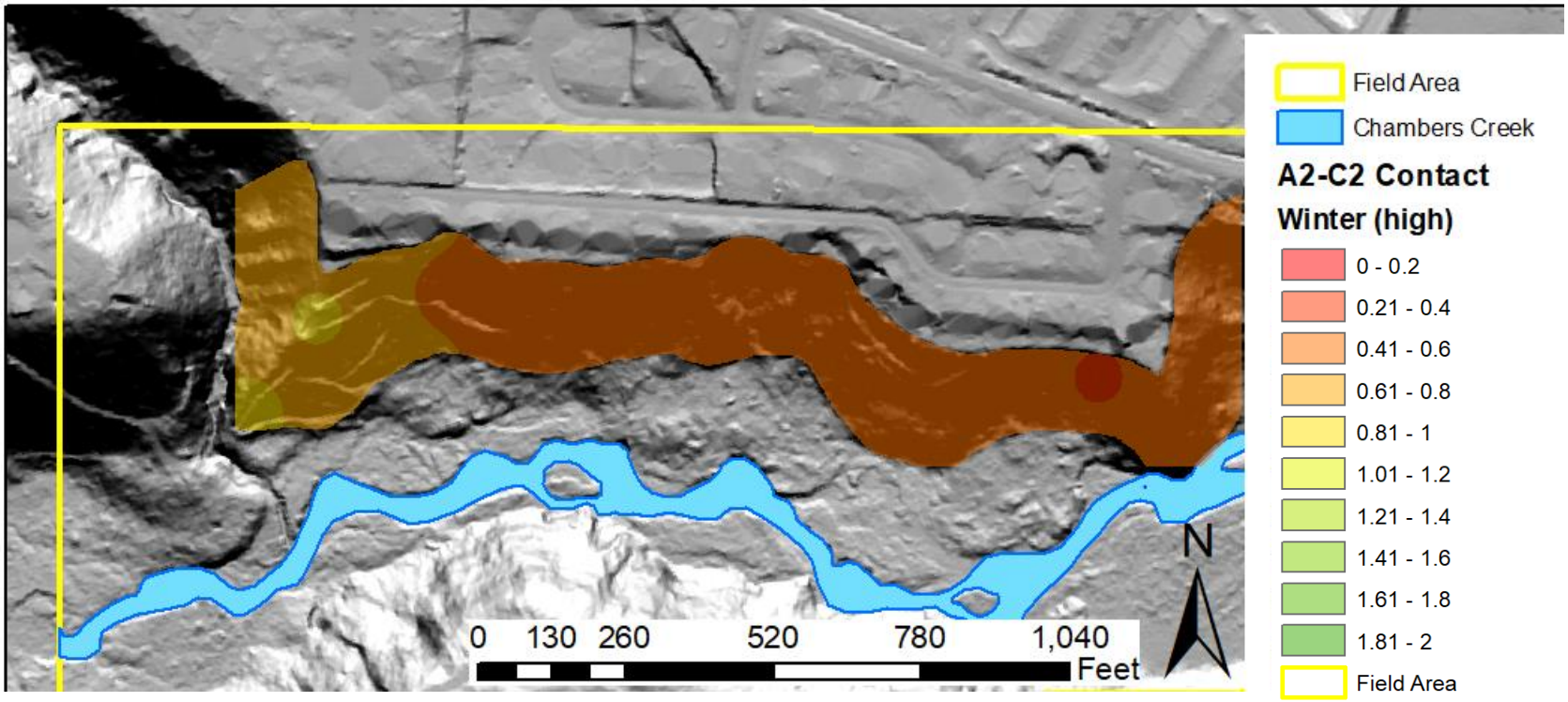

Figure 13: Field area shallow-seated Factor of Safety Model for high scenario (winter flow) along the A2-C2 contact.

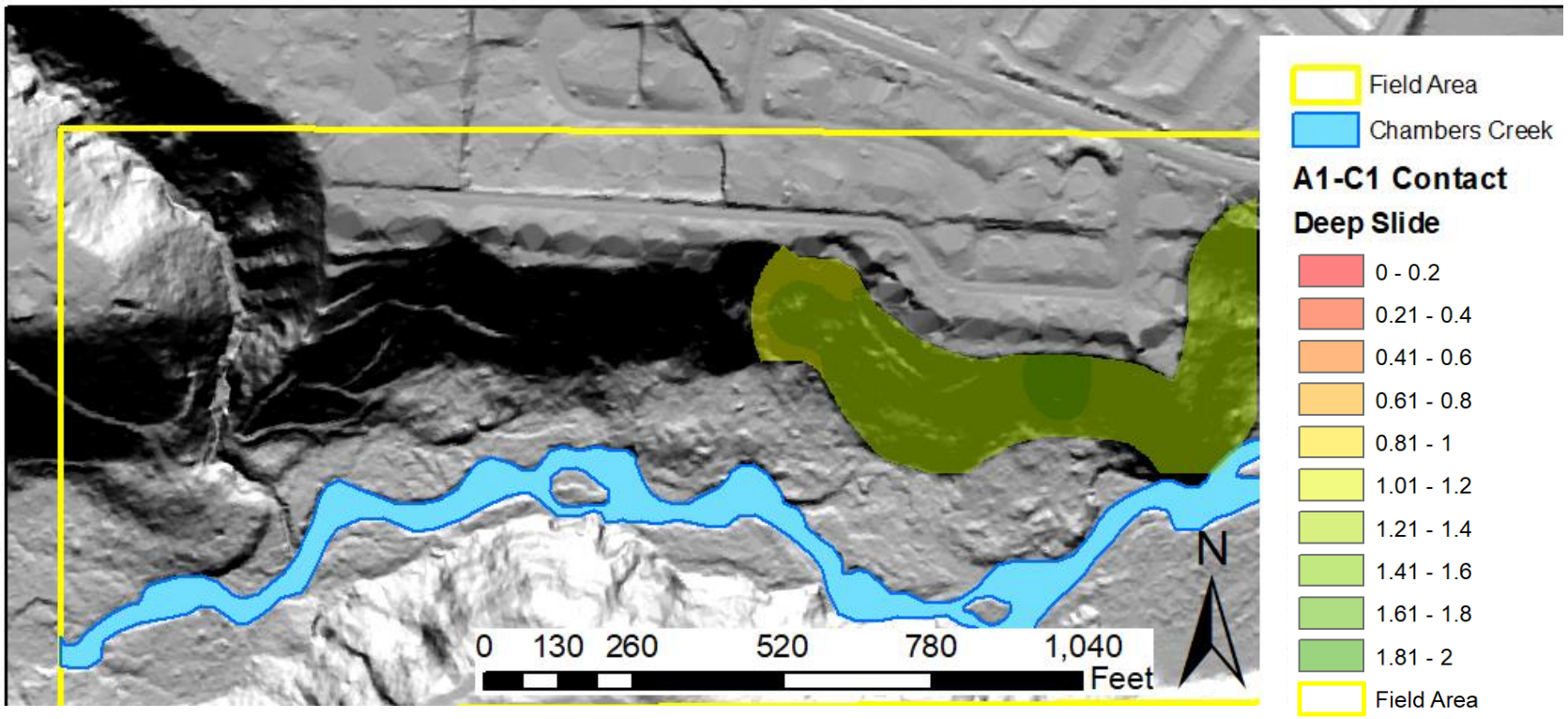

Figure 14: Field area deep-seated Factor of Safety Model along the A1-C1 contact. Since this model is based on a landslide failure occurring on the A1-C1 susceptible geologic contact, the data ends where the contact reaches the top of the terrace.

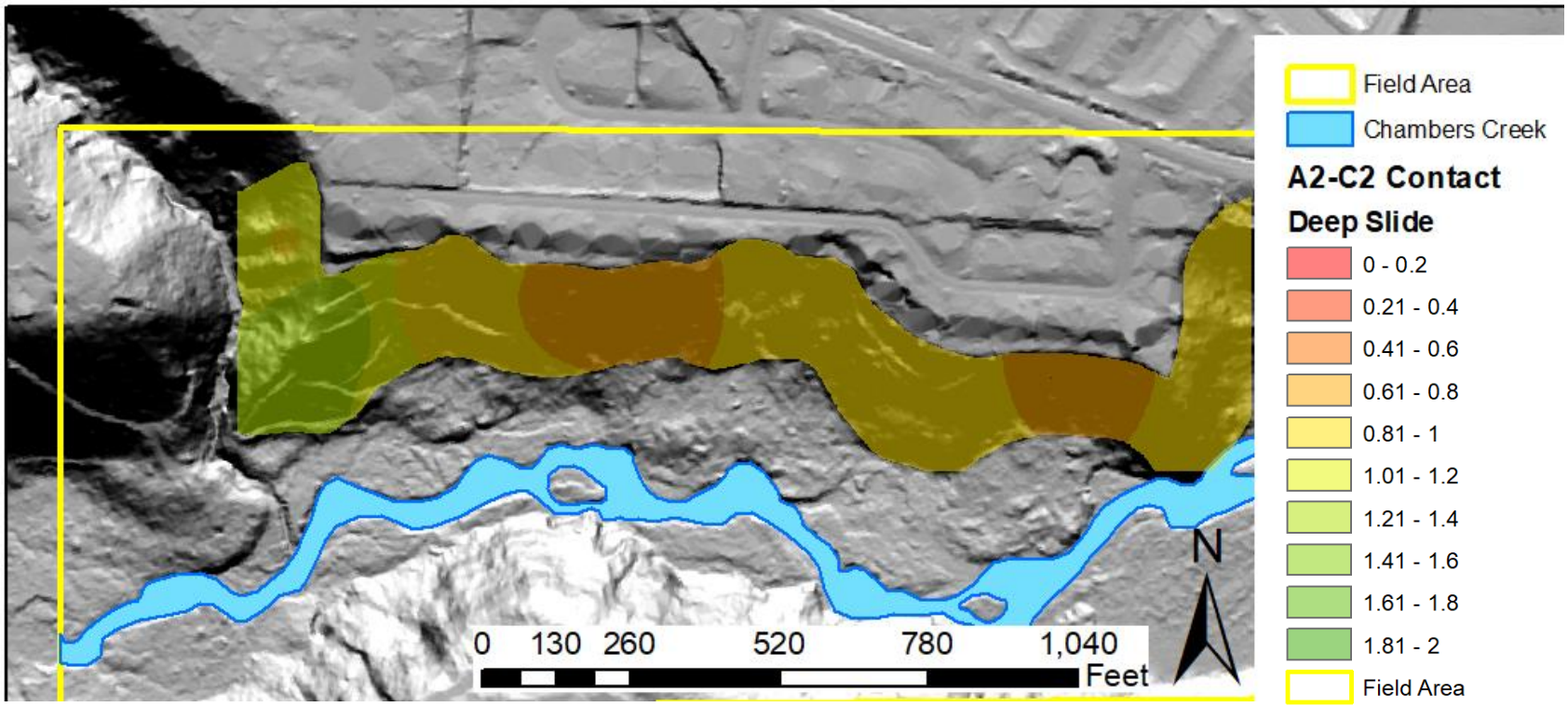

Figure 15: Field area deep-seated Factor of Safety Model along the A2-C2 contact.

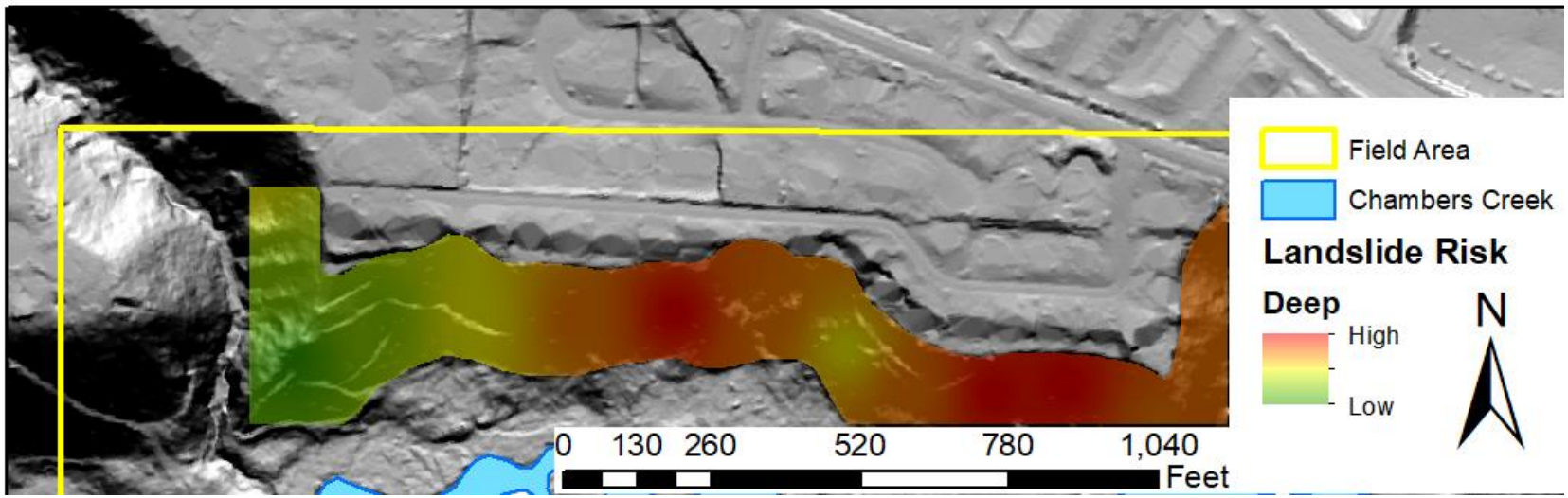

Figure 16: Image showing deep-seated landslide risk in field area based on landslide scarps, easterly dip of units, and factor of safety models.

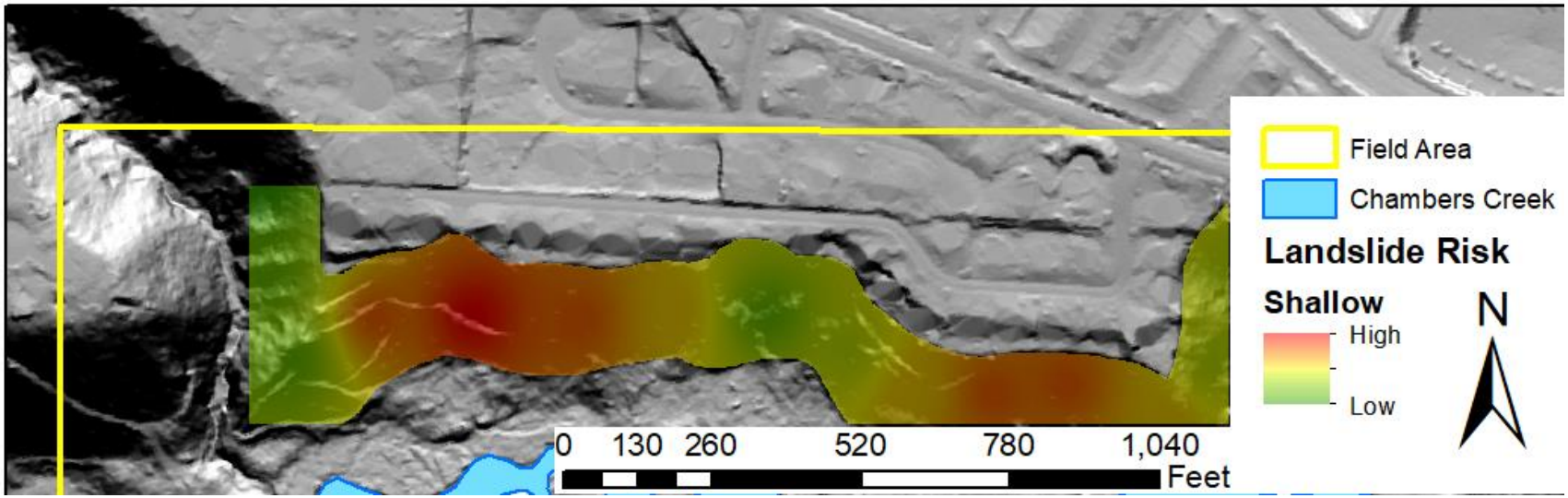

Figure 17: Image showing shallow landslide risk in field area based surface SPT values, surface slopes, NDVI vegetation type, and field observation